Integrating direct air capture with small modular nuclear reactors

Document Version:
Publisher's PDF, also known as Version of Record (includes final page, issue and volume numbers)

Please check the document version of this publication:

• A submitted manuscript is the version of the article upon submission and before peer-review. There can be important differences between the submitted version and the official published version of record. People interested in the research are advised to contact the author for the final version of the publication, or visit the DOI to the publisher's website.
• The final author version and the galley proof are versions of the publication after peer review.
• The final published version features the final layout of the paper including the volume, issue and page numbers.

Link to publication

PAPER • OPEN ACCESS

Integrating direct air capture with small modular nuclear reactors: understanding performance, cost, and potential

To cite this article: Luca Bertoni *et al* 2024 *J. Phys. Energy* **6** 025004

View the article online for updates and enhancements.

Journal of Physics: Energy

PAPER

Integrating direct air capture with small modular nuclear reactors: understanding performance, cost, and potential

Luca Bertoni[1], Simon Roussanaly[2], Luca Riboldi[2], Rahul Anantharaman[2] and Matteo Gazzani[1,3,*]

[1] Copernicus Institute of Sustainable Development, Utrecht University, Princetonlaan 8a, Utrecht 3584 CB, The Netherlands
[2] SINTEF Energy Research, Postboks 4761 Torgarden, Trondheim 7465, Norway
[3] Eindhoven University of Technology, Eindhoven 5612 AP, Netherlands
[*] Author to whom any correspondence should be addressed.

E-mail: m.gazzani@uu.nl and m.gazzani@tue.nl

Abstract

Direct air capture (DAC) is a key component in the transition to net-zero society. However, its giga-tonne deployment faces daunting challenges in terms of availability of both financial resources and, most of all, large quantities of low-carbon energy. Within this context, small modular nuclear reactors (SMRs) might potentially facilitate the deployment of DAC. In the present study, we present a detailed thermodynamic analysis of integrating an SMR with solid sorbent DAC. We propose different integration designs and find that coupling the SMR with DAC significantly increases the use of thermal energy produced in the nuclear reactor: from 32% in a stand-alone SMR to 76%–85% in the SMR-DAC system. Moreover, we find that a 50–MW SMR module equipped with DAC could remove around 0.3 $MtCO_2$ every year, while still producing electricity at 24%–42% of the rated power output. Performing a techno-economic analysis of the system, we estimate a net removal cost of around 250 €/tCO_2. When benchmarking it to other low-carbon energy supply solutions, we find that the SMR-DAC system is potentially more cost-effective than a DAC powered by high-temperature heat pumps or dedicated geothermal systems. Finally, we evaluate the potential of future deployment of SMR-DAC in China, Europe, India, South Africa and the USA, finding that it could enable up to around 96 $MtCO_2$/year by 2035 if SMRs prove to be cost-competitive. The impact of regional differences on the removal cost is also assessed.

1. Introduction

In order to limit the temperature increase due to global warming to well below 2 °C compared to the pre-industrial levels, carbon dioxide removal (CDR) must be implemented at giga-tonne scale alongside the reduction of anthropogenic emissions [1, 2]. According to the National Academy of Sciences [3], the carbon removal rate should reach multiple $GtCO_2$/year by mid-century and increase further by the end of the century. Among the available CDR technologies, direct air capture (DAC) is amongst the ones with the highest carbon mitigation potential [4] and the Net-Zero Emissions by 2050 roadmap developed by the International Energy Agency (IEA) estimates that DAC technologies should remove 90 $MtCO_2$/year by 2030 and 985 $MtCO_2$/year by 2050 [5].

Currently, two main commercial DAC solutions exist: solvent-based DAC (developed by, e.g. Carbon Engineering [6]) and sorbent-based DAC (developed by, e.g. Climeworks [7]). Both types of DAC require a considerable amount of thermal and electrical energy, typically in an 80–20 ratio [8]. However, the temperature needed for the regeneration of the active material differs significantly between the two technologies, with solvent-based DAC requiring around 900 °C and solid sorbent DAC requiring temperatures in the range of $100 - 200°$. For this reason, the latter allows for the use of waste process heat or heat provided at relatively low temperatures by low-carbon energy sources, such as geothermal and nuclear plants [8].

Another important technology for a secure and resilient supply of low-carbon energy in the energy transition is nuclear fission [9]. In the last years, interest has grown around small modular reactors (SMRs), with more than 70 SMR designs under development for different applications [10]. SMRs are defined by the International Atomic Energy Agency as 'newer generation reactors designed to generate electric power typically up to 300 MW, whose components and systems can be shop fabricated and then transported as modules to the sites for installation' [10]. Given the enhanced passive safety features and the smaller size, these reactors can be co-sited with other activities and appear to be particularly suited alongside non-electric applications. One of these applications could potentially be direct air carbon capture. Especially, coupling SRMs with DAC could be advantageous from a system perspective. Firstly, in the future DAC might have to compete for low-carbon electricity with processes for green hydrogen [11] or industrial electrification [12]. As such, developing different types of energy supplies is important to ensure that the development of DAC will not be hindered by clean energy availability constraints. Secondly, in contrast to other low-carbon technologies that are to some extent location-dependent (wind, solar and geothermal energy), powering DAC with an SMR would allow the building of the facility near a CO_2 storage site, lowering the costs of CO_2 transport. Despite these considerations, little is known about the use of SMRs as energy providers to DAC.

Building upon the development of Climeworks, multiple papers have recently investigated the integration of a solid sorbent DAC with geothermal sources (e.g. [8, 13, 14]). On the other hand, to the best of our knowledge, only two articles researched the potential synergies between DAC and nuclear fission ([8, 15]). McQueen *et al* [8] coupled a 1 GW_e Westinghouse pressurized-water reactor with DAC. In their work, they performed an economic analysis assuming that 5% of the steam is spilt from the main steam generator and diverted to the DAC. More recently, Slesinski and Litzelman [15] assessed the potential economic benefits of co-siting a DAC plant with an SMR, concluding that providing low-grade heat to the DAC could benefit the economics of the SMR. However, in their analysis, they considered a generic model (in type and size) of SMR and did not consider the temperature profile of the thermal demand of DAC. Moreover, they approached the analysis from the perspective of the SMR owner, thus without looking at how using the SMR as an energy supply would affect the cost of removing CO_2 with the DAC. Next to these two papers, a recent technical report from the United States Department of Energy [16] analyzed the performance and the market outlook of nuclear energy used to power DAC. It was found that a 'nuclear-DAC system provides economic benefits when compared to non-nuclear DAC systems'.
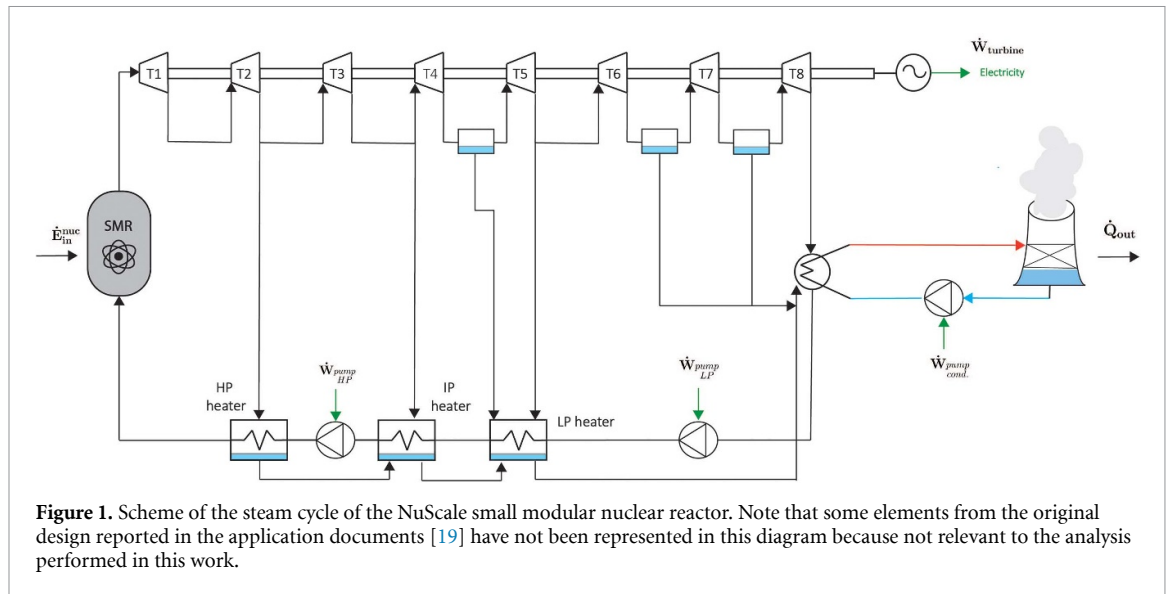
Therefore, while studies exist that investigate the coupling of large-scale nuclear reactors with DAC, to the best of our knowledge this is the first scientific work where the coupling with small modular nuclear reactors (SMRs) is considered from a detailed techno-economic perspective. Worth mentioning is that significant differences exist in the steam cycle of a small and a large nuclear reactor, which therefore result in different integration schemes with the DAC heat supply fluid. In addition, the benchmarking of the SMR-DAC option against other low-carbon sources has not been investigated.

With this work, we provide a comprehensive thermodynamic analysis of the SMR-DAC integration which includes the full SMR steam cycle and the thermal profile of the DAC demand. In this way, we aim to quantify the potential synergy between SMR and DAC from an energy perspective. Furthermore, using thermodynamic analysis, we assess the net CO_2 removal cost of the system and we show how it compares with other three options that could be used to power DAC. Finally, we estimate the future potential of the system in terms of CO_2 removal capacity that could be achieved when considering different scenarios of SMR deployment. To this end, we also show how the CO_2 removal cost changes with location.

2. Technical analysis of SMR-DAC coupling

2.1. SMR technology and model
The SMR considered in this work is the NuScale SMR from the American company NuScale Power, LCC. This model is a light-water-cooled pressurized-water reactor with an integral design, meaning that the reactor core and primary cooling loop are contained within a single reactor vessel. We chose this specific reactor because NuScale Power submitted the application for design certification to the United States Nuclear Regulatory Commission (USNRC) on 31 December 2016 and received the design certification 6 years later in January 2023 [17]. In addition to the technology readiness level, having undergone the regulatory review, detailed technical information on the SMR is publicly available from the website of the USNRC [18]. In particular, the 'Steam and power conversion system' chapter [19] provides the technical information that is needed for this research: a detailed block flow diagram of the power conversion system (figure 1) and a thorough presentation of each block with relevant data about the steam system design. Currently, one NuScale module is designed to have a power output of 77 MW of electricity (MW_e) [20]. However, this is the result of a power increase from the design submitted for approval in 2016, which is 50 MW_e. Since the most detailed technical information available is for the 50 MW_e design, this is the design used in this work. This

Figure 1. Scheme of the steam cycle of the NuScale small modular nuclear reactor. Note that some elements from the original design reported in the application documents [19] have not been represented in this diagram because not relevant to the analysis performed in this work.

preliminary choice influences the maximum carbon removal rate per module, as it scales directly with the rated power of the SMR, but it will not significantly change the overall thermodynamic integration as long as the steam cycle design parameters are maintained.

In this work, the reference steam cycle of the SMR together with all the relevant physical (mass flow) and thermodynamic parameters (pressure and specific enthalpy) in every point of the system[4] are taken from [19]. When integrating the SMR with DAC (see section 2.3), some of the steam is spilt from the steam cycle of the nuclear reactor, thus changing the mass flows. While this happens, we consider the thermodynamic properties of the SMR cycle to remain as provided by the application document. For example, the isentropic efficiency of turbines is considered to be constant, even though its value varies depending on the amount of steam flowing through the turbine. This is of course a (minor) simplification, which we believe to be acceptable for the scope of the analysis.

The SMR model consists of 3 main steps: *(i)* calculating all the relevant mass flows (including the ones going to the DAC to provide the necessary thermal energy, see section 2.3), *(ii)* calculating the power used to run the pumps, and finally *(iii)* obtaining the net power output of the SMR module. The method behind these calculations is explained in detail in the supplementary information.

2.2. Solid sorbent DAC process

The other main element of the process is the DAC unit. As mentioned in the introduction, the DAC system analyzed is solid sorbent-based. This technology is characterized by two main stages, adsorption and desorption, which are performed successively and cyclically repeated. As it is illustrated in figure 2, in the adsorption phase the ambient air is forced into an air contactor, where CO_2 is selectively removed through the solid sorbent; CO_2-lean air leaves the contactor and goes back to the environment. In the desorption phase, firstly vacuum is created, while the sorbent is preheated by means of an external heating fluid. The product of this phase is nitrogen-rich and therefore released into the environment. Secondly, the sorbent is further heated up to the maximum desorption temperature; the CO_2 released from the solid sorbent is captured and sent to a compression stage after drying. Finally, prior to the restart of the adsorption step, the sorbent is cooled to ambient temperature (typically with direct flow of air).

The resulting cycle is called vacuum-temperature swing adsorption, because of the driving forces used to regenerate the sorbent. Even though solid sorbents could theoretically be regenerated by exploiting either a temperature or a pressure difference, these are not practically viable given the low concentration of CO_2 in the air, lest going to very high temperatures or deep vacuum conditions.

The performance of DAC is influenced by the chemical and physical properties of the sorbent. Many types of sorbents have been proposed; Sabatino *et al* [21] analyzed four different types of sorbents and, since none of these can be regarded as winning reference, they proposed to evaluate DAC with an exemplary sorbent combining the equilibrium data of the four materials. Similarly, in this work, the performance of the DAC system is computed considering the exemplary sorbent. Details about the relevant parameters of the DAC can be found in the supplementary information.

---

[4] The values reported are site-dependent, as they are affected by external environmental conditions.
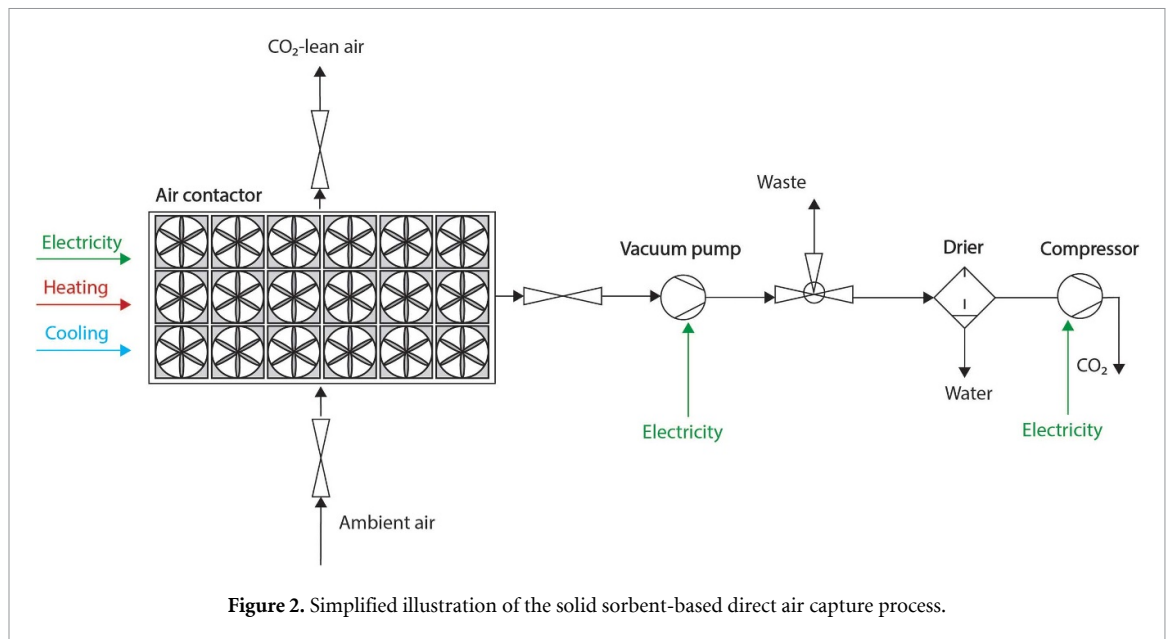
Figure 2. Simplified illustration of the solid sorbent-based direct air capture process.

2.3. Layout of SMR-DAC system

In order for the SMR to provide the necessary thermal and electrical power to the DAC, the two systems need to be properly integrated[5]. In particular, one or more heat exchangers are required to transfer the energy from the steam to a heat transfer fluid, which in turn heats up the DAC modules. Therefore, the integration consists of two stages: the delivery of heat from the SMR to the heat transfer fluid, and the delivery of heat from the transfer fluid to the DAC unit. The supply of heat can be designed in multiple ways. In this work, two layouts are considered:

1. *High energy integration design (HEI)*: the aim is to minimize the power output loss of the SMR module per unit of thermal energy delivered to the DAC. To do so, the regeneration of the solid sorbent is divided into 6 steps with increasing temperatures in subsequent time steps, which allows the integration of heat below the maximum temperature of the DAC regeneration (similar to a counter-current heat exchanger).
2. *Low energy integration design (LEI)*: the objective of the LEI approach is to reduce the engineering required to integrate the SMR module and the DAC. In this configuration, the steam temperature is never below the maximum DAC regeneration temperature; therefore, the amount of steam is independent of the DAC regeneration profile and only dependent on the maximum temperature, the pinch point, and the total regeneration energy.

In both layouts, a minimum mass flow rate of 15% is maintained in each stage of the turbine to ensure stable and safe operation. Moreover, the following assumptions regarding the heat exchangers have been made. Firstly, the steam-heat transfer fluid heat exchangers are designed as counter-current. Secondly, pressure losses in heat exchangers are neglected; this implies that we do not account for the (minor) work required by circulation pumps and that heat transfer happens at constant pressure. Thirdly, by design, a temperature difference of $\Delta T_{min} = 10\,°C$ between the hot stream inlet and the cold stream outlet is assumed. Finally, the cold and hot streams exit the heat exchanger at the same temperature.

2.3.1. HEI design

As is shown in figure 3, the steam is spilt at six different thermodynamic conditions—here defined by pressure (p) and specific enthalpy (h) - from the last six stages of the SMR turbine (from T3 to T8). Each of these streams is diverted to a dedicated heat exchanger, where the energy is delivered to the heat transfer fluid. More specifically, the fluid is heated up until the temperature $T_i - \Delta T_{min}$, where T_i is the temperature of the steam from the turbine stage *i*. This holds for every heat exchanger but the first, where the heat transfer fluid is heated up until the maximum desorption temperature of the DAC process T_{max}[6] plus ΔT_{min} (see the T–Q diagram in figure 6(a)).

---

[5] The integration might pose regulatory challenges. These are not evaluated here as they are beyond the scope of this work.
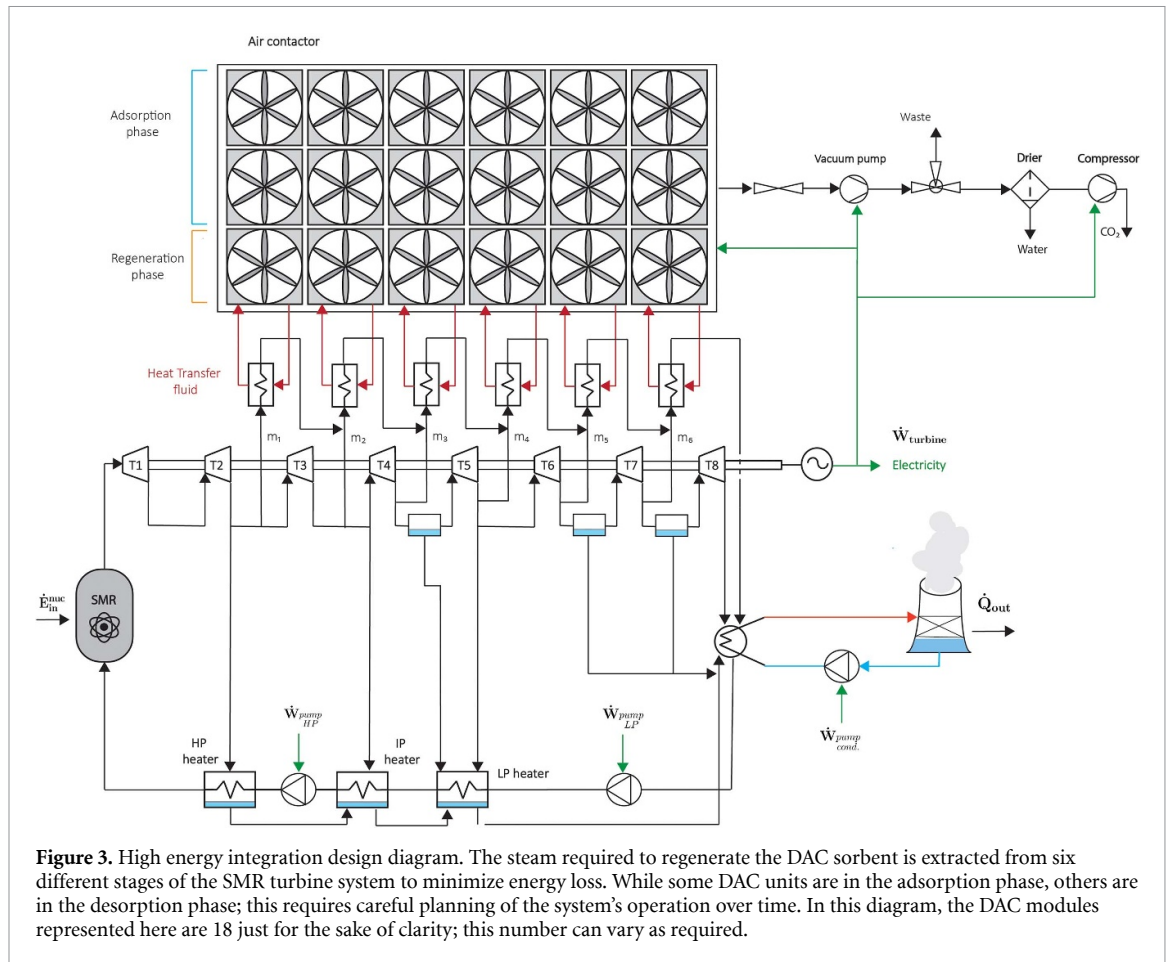[6] In this work, $T_{max} = 127\,°C$.

Figure 3. High energy integration design diagram. The steam required to regenerate the DAC sorbent is extracted from six different stages of the SMR turbine system to minimize energy loss. While some DAC units are in the adsorption phase, others are in the desorption phase; this requires careful planning of the system's operation over time. In this diagram, the DAC modules represented here are 18 just for the sake of clarity; this number can vary as required.

After exiting the heat exchanger, the cold steam *i* is injected into the hot steam coming out of the next turbine *i+1*. In the last stage, the steam is returned via piping to the SMR, where it rejoins the exhaust steam from the turbines and is sent to the condenser. The six streams of hot heat transfer fluid are sent to the DAC unit. It is worth noting that each stream of heat transfer fluid *i* heats up the solid sorbent only up to the maximum temperature of the heat transfer fluid *i* minus $\Delta T_{\max}$. Therefore, given the cyclic nature of the DAC unit, the system needs to be operated in such a way that every DAC module receives each of the 6 streams of heat transfer fluid consecutively in time. This requires careful optimization of the delivery of heat to the DAC modules over time, increasing the complexity of the system, but also allowing for providing heat under a limited temperature difference. Therefore, HEI should be regarded as the configuration where the maximum theoretical heat integration is achieved.

2.3.2. LEI design
In the LEI design (figure 4), the heat demand of the DAC is entirely supplied using steam at a temperature higher than the maximum desorption temperature. As it can be noticed from figure 4, the steam required is spilt from the third stage of the turbine system and sent to one heat exchanger. Here, the heat transfer fluid is heated up to $T_{\max} + \Delta T_{\min}$, so the heat transfer fluid is able to deliver all the heat necessary to fully regenerate the sorbent and go back to the heat exchanger at a temperature of $T_{\max} = 127\,^{\circ}\mathrm{C}$ (see figure 6(a)).

This design significantly reduces the complexity of the integration, as the heat transfer fluid is sent to the DAC unit always at the same temperature, with no particular care of the time of the DAC cycle. In addition, it requires only one extra heat exchanger for the integration, compared to the 6 needed for the HEI design. Accordingly, LEI should be regarded as the least energy-integrated system.

2.4. Resulting energy and mass balances
An overview of the power balance of the SMR-DAC process—low and HEI—is shown in figure 5, while specific numbers are reported in table 1. The integration of DAC with an SMR cycle increases the energy use of the available thermal energy from the nuclear reactor substantially. While the SMR as a stand-alone system converts around one-third of the nuclear energy into a useful output—in this case electricity, this share more than doubles when DAC is added and CO_2 is co-produced along with electricity (76%–85% for LEI and HEI

Figure 4. Low energy integration design diagram. Here, the steam is extracted at one temperature. This temperature is greater than the maximum desorption temperature of the solid sorbent so that the entire thermal demand of DAC can be covered. The DAC modules represented here are 18 as an example; this number can vary as required.
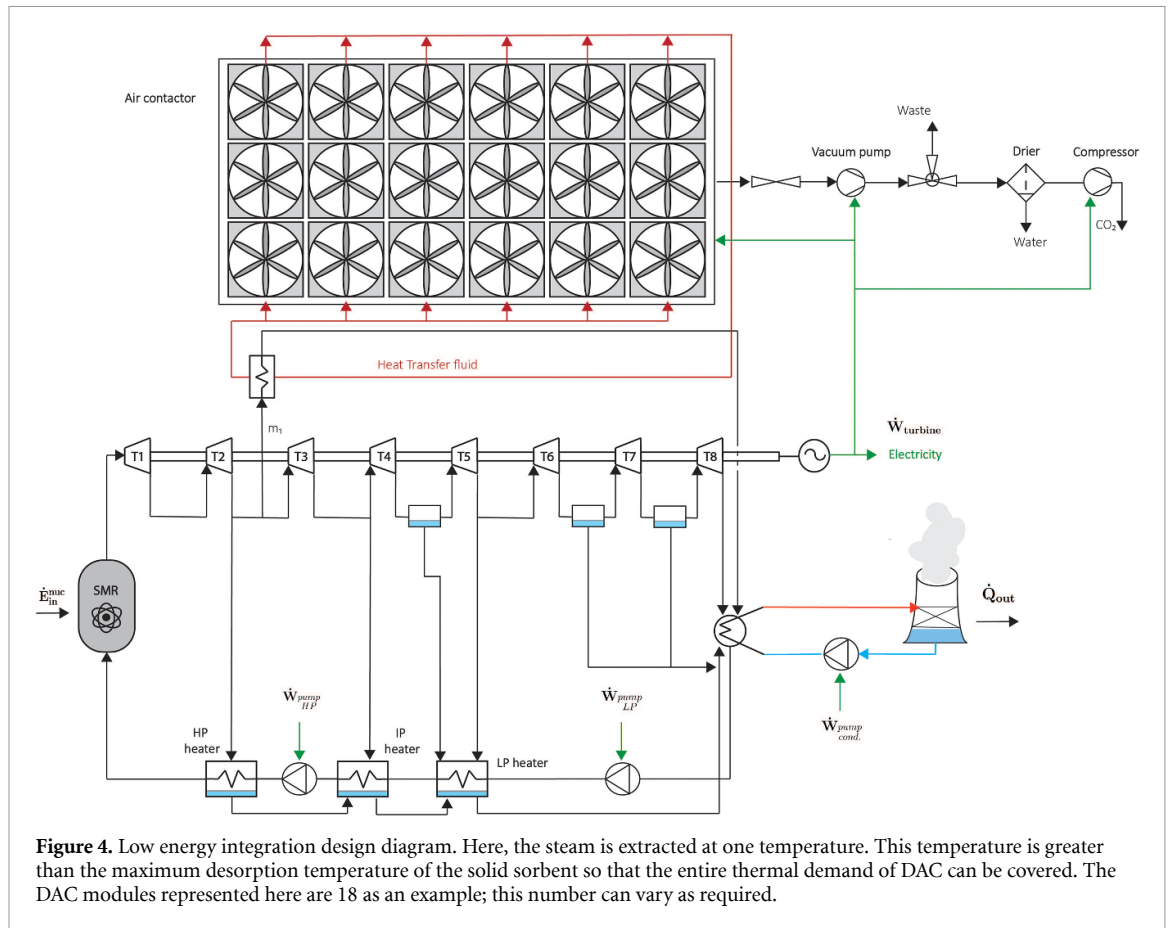
respectively). On the other hand, while the total energy use increases, the electricity production slightly decreases and the waste heat is reduced significantly. This is possible thanks to the fact that the thermal energy demand of DAC can be covered entirely with low-grade heat, which is particularly abundant in a Rankine cycle for nuclear plants. It should, however, be noted that more than half of the electricity production is not dispatched to the grid but rather used to run the DAC units (mostly for blowers). Depending on the specific local conditions, this might even be a good proposition for the SMR owner, for example in the case of a congested market with a high share of renewables. As such, one 51-MW_e SMR module can remove 0.32–0.34 $MtCO_2$ per year[7], which translates into 3.8–4.1 $MtCO_2$ when a plant with 12 SMRs is considered (which is one of the standard designs proposed by NuScale). At the same time, the system can still produce 24%–41% of the rated electrical power output of the nuclear reactor for injection in the electricity grid (see table 1 for more details).

Alongside the exergy loss, the *loss factor* ϕ, defined as the amount of electricity lost per unit of heat supplied to the DAC (MW_e/MW_{th}), provides a quantitative indication of how efficiently the thermal power from the steam cycle is transferred to the DAC. Since the electric power generated by the SMR decreases linearly with the thermal power supplied to the DAC in both the HEI and LEI design (see figure 6(b)), the loss factor is constant. The two designs show a loss factor of $\phi_{HEI} = 0.14$ and $\phi_{LEI} = 0.24$ respectively, meaning that the HEI design almost halves the power output loss compared to the LEI. In addition, the model identifies the maximum thermal load that can be supplied to the DAC: 98 MW_{th} for the HEI design and 92 MW_{th} for the LEI design. These values set the maximum number of DAC modules that can be installed and thus the maximum annual removal rate per SMR module.

Overall, the HEI and LEI designs represent respectively the maximum energy integration achievable and the simplest integration design. While the HEI design outperforms the LEI design in terms of efficient use of the available energy, its complex design might make it look unattractive for a real-case implementation of the SMR-DAC system. Therefore, the actual implementation of an SMR-DAC system might be based on a design that lies in between the HEI and LEI design in terms of energy performance and complexity of the integration. For example, the steam could be extracted at two different temperatures instead of six (HEI

---

[7] Assuming 85% utilization rate (percentage of hours operating at maximum capacity).

Figure 5. Energy balance of the SMR (left) and the two proposed layouts for the integration of SMR and DAC. Values are per one SMR module. Wasted heat refers to the heat rejected by the system at the condenser. The diagram shows that coupling the nuclear reactor with DAC reduces the amount of electricity that can sold to the grid, but it greatly increases the usage of the thermal energy produced by the reactor.
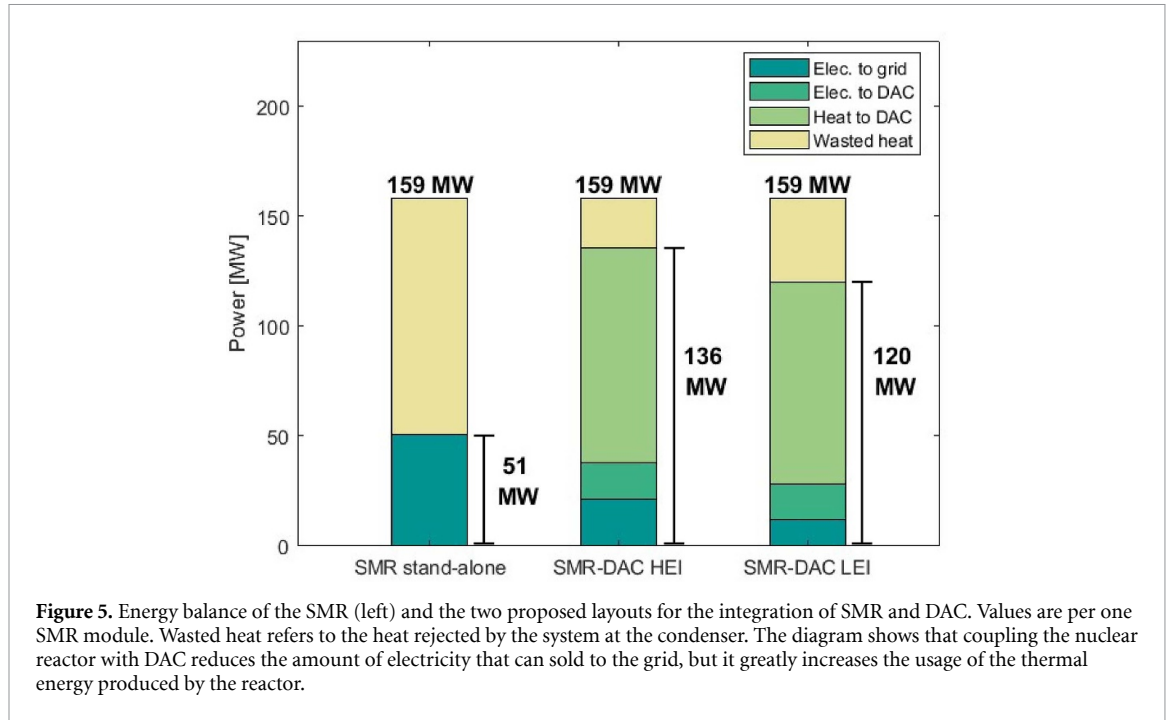
Table 1. Model results when there is no DAC integrated with the SMR (*SMR*) and when the maximum DAC capacity is installed (*SMR-DAC HEI* and *SMR-DAC LEI*). The symbol $\dot{X}$ stands for the exergy content of heat. Values are per one SMR module.

		SMR	SMR-DAC HEI	SMR-DAC LEI
$\dot{E}_{in}^{nuc}$ (MW$_{th}$)		159.0	159.0	159.0
$\dot{W}_{pumps}$ (MW$_e$)		0.8	0.5	0.6
$\dot{Q}$ ($\dot{X}$) to DAC (MW$_{th}$)		– (–)	98.0 (20.0)	92.0 (35.3)
$\dot{W}$ to DAC (MW$_e$)		—	16.7	16.1
$\dot{W}$ to grid (MW$_e$)		50.7	21.1	12.2
Heat rejection (MW$_{th}$)		107.5	22.7	38.1
Loss factor (MW$_{el}$/MW$_{th}$)		—	0.14	0.24
Energy use (%)		32	85	76
	m$_1$	—	5.1	44.0
	m$_2$	—	6.2	—
Mass Extraction (kg s^{-1})	m$_3$	—	18.9	—
	m$_4$	—	4.9	—
	m$_5$	—	3.6	—
	m$_6$	—	4.4	—
DAC units installed per SMR module		—	1475	1380
Removal Rate per SMR module (MtCO$_2$/year)		—	0.34	0.32
Removal Rate per MW$_{th}$ (ktCO$_2$/year/MW$_{th}$)		—	2.1	2.0

design) or one (LEI design), making this design more energy efficient than the LEI design, but less than the HEI; similarly, it would be more complex than the LEI, but less than the HEI.

Next to this, the analysis showed that removing CO_2 might require a significant share of the electrical power output of the SMR depending on the preferred removal rate. However, it is worth stressing that the CO_2 produced from the air is an additional, if not the main, valuable product that the SMR-DAC plant produces along with electricity—and not a requirement to comply with emissions mitigation as in carbon capture from fossil-based point sources. Therefore, the optimal operating point in terms of electricity and CO_2 production will vary in time and will depend on the local market value of electricity and CDR credits. In other words, a strong penalization of the electricity output might still coincide with the optimal (economic) operation strategy.
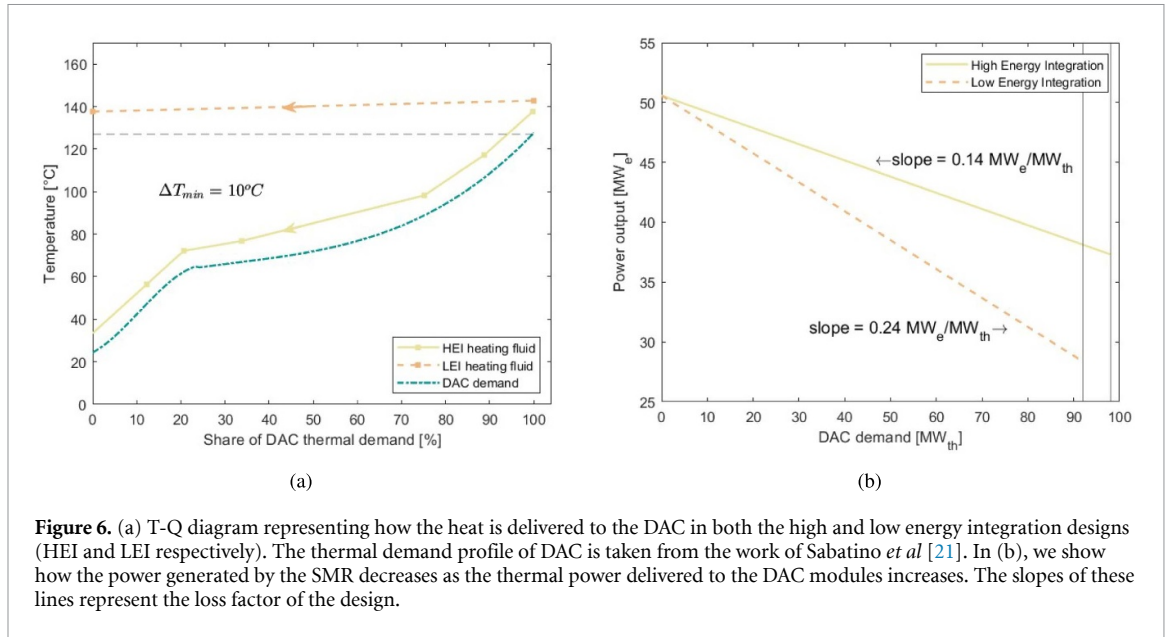
Figure 6. (a) T-Q diagram representing how the heat is delivered to the DAC in both the high and low energy integration designs (HEI and LEI respectively). The thermal demand profile of DAC is taken from the work of Sabatino *et al* [21]. In (b), we show how the power generated by the SMR decreases as the thermal power delivered to the DAC modules increases. The slopes of these lines represent the loss factor of the design.

3. Comparative techno-economic analysis and global potential

In this section, the net removal cost (NRC) of the SMR-DAC system is calculated for both layouts (HEI and LEI) and compared to three other options of energy supply for DAC:

1. High-temperature heat pump (HP) with electricity from the grid (Case *HP*)
2. Enhanced geothermal for the supply of DAC heat plus electricity from the grid (Case *GeoHeat*)
3. Geothermal power plant for both electricity and heat supply, where heat is a waste from the plant (i.e. it does not affect electricity) (Case *GeoWaste_el*)

Figure 7 shows how the comparative analysis is structured.
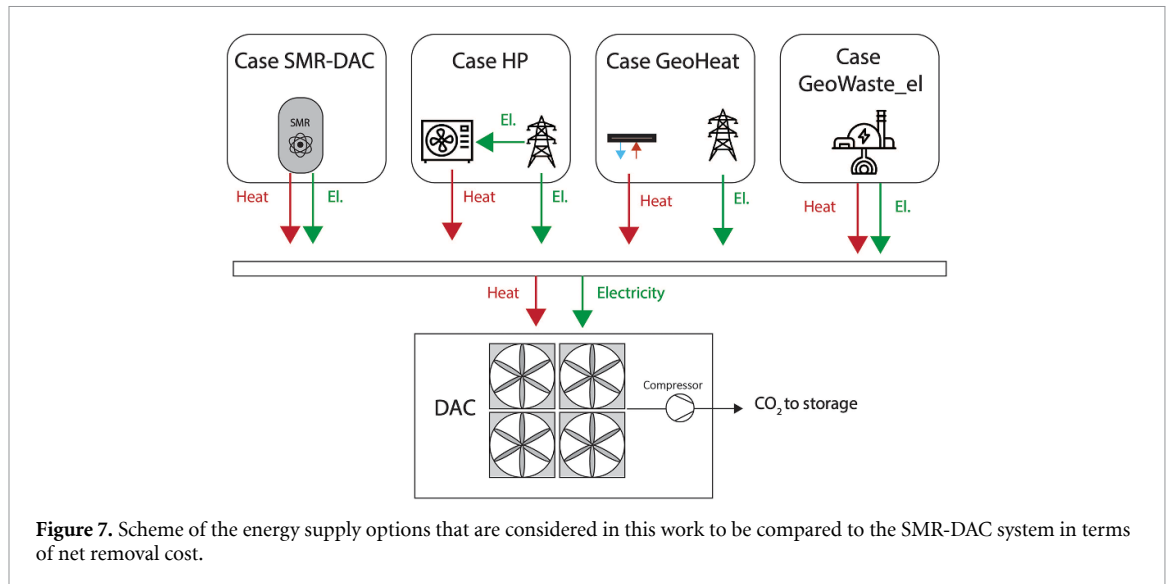
3.1. Methods and data
The NRC is calculated as

$$NRC = \frac{\alpha \ (CAPEX_{\text{DAC}} + CAPEX_{\text{int}}) \ + \ O\&M_{\text{DAC}}^{\text{fixed}} \ + D_{\text{th}} \ p_{\text{heat}} + D_{\text{el}} \ p_{\text{el}}}{m_{\text{CO}_2}} + \theta_{\text{sorbent}} \qquad (1)$$

where α is the capital recovery factor, $CAPEX_{\text{DAC}}$ and $CAPEX_{\text{int}}$ are the capital cost for the DAC and the integration of SMR and DAC respectively; $O\&M_{\text{DAC}}^{\text{fixed}}$ are the fixed operation and maintenance costs; D_{th} and D_{el} are the specific thermal and electrical energy demand of DAC; p_{heat} and p_{el} are the heat and electricity price; m_{CO_2} is the net CO_2 removed in one year; θ_{sorbent} is the cost for replacing and disposing the sorbent per unit of net CO_2 removed. In the SMR-DAC system, the cost of heat (p_{heat}) is assumed to be equal to the opportunity cost that the SMR faces when it supplies heat to the DAC instead of selling the equivalent electric power to the grid, which is influenced by the loss factor of the design ϕ_{design}. Therefore, we have

$$p_{\text{heat}} = p_{\text{el}} \ \phi_{\text{design}}. \qquad (2)$$

When electricity is purchased from the grid, the associated indirect emissions are considered in the NRC by subtracting them from the total CO_2 removed. For each case, the techno-economic parameters of the DAC, the electricity price and the discount rate are kept constant. The variables that determine the change in NRC are the cost of heat (see table 2), the emissions related to energy use and the capital cost for the integration of the DAC and the energy supply. More details about each system can be found in the supplementary information.

Figure 7. Scheme of the energy supply options that are considered in this work to be compared to the SMR-DAC system in terms of net removal cost.

Table 2. Cost of heat for each DAC system.

	Cost of heat (€/MWh)
SMR-DAC HEI	5.9
SMR-DAC LEI	11.3
HP	39.6
GeoHeat	30.3
GeoWaste_el	0

Table 3. Relevant economic parameters.

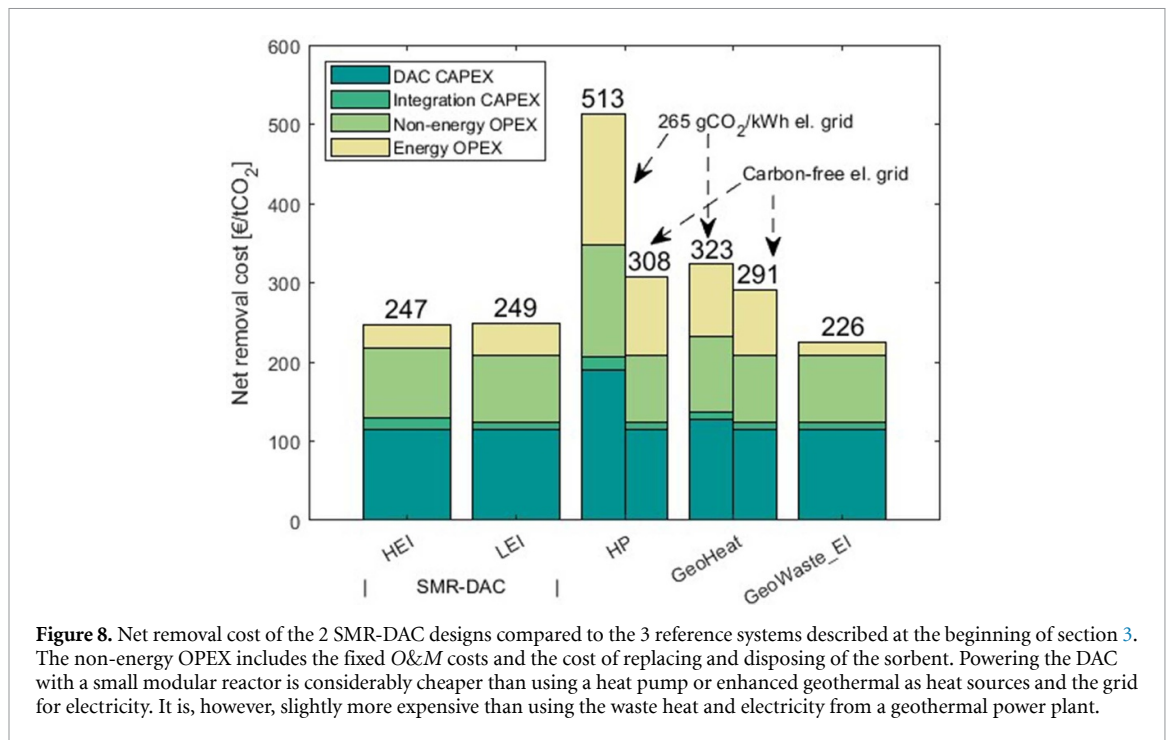| Parameter	Symbol	Unit	Value
CAPEX DAC	$CAPEX_{DAC}$	M€/MtCO$_2$/year	1226
CAPEX integration	$CAPEX_{int}$	M€/MtCO$_2$/year	100
Opex DAC	$O\&M_{DAC}$	% of CAPEX/year	6
Cost of sorbent	$\theta_{sorbent}$	€/tCO$_2$	5
Lifetime DAC	l_{DAC}	years	25
Discount rate	r	%	8
Electricity price	p_{el}	€/MWh	45

The other economic parameters[8] used in this work are reported in table 3. The capital and non-energy operating costs of DAC are taken from [22][9]. For the integration cost, which is added to the capital cost of DAC in all the cases considered, a value of 100 €/MtCO$_2$/year is assumed. For the HEI design of SMR-DAC, this value is multiplied by 1.5 to take into account the greater complexity required compared to other cases. These are of course estimates based on intuition, and therefore subject to possibly significant variation. They are however expected to play a minor role in the economics of the plant and in line with a preliminary cost assessment.

3.2. NRC

The SMR-DAC system shows an NRC of around 250 €/tCO$_2$ (see figure 8) for both the HEI and LEI design (247 €/tCO$_2$ for HEI, 249 €/tCO$_2$ for the LEI). This cost is mainly driven by the CAPEX and O&M costs of the DAC, which account for more than 200 €/tCO$_2$. The integration costs have a minor role, contributing to the NRC with 14 €/tCO$_2$ in the HEI design and 9 €/tCO$_2$ in the LEI design. The better energy integration of the HEI design leads to energy costs that are 24% lower compared to the LEI design. Overall, the NRC of the two designs is very similar. However, as shown in table 1, the HEI design can deliver more negative emissions

---

[8] In this work, all the monetary values are adjusted for inflation to the value of € in 2021. For the conversions from other currencies to €, the database of the European Central Bank is used.
[9] Values refer to the case OB-EB in [22], from which are excluded all the costs not related to the DAC plant. For the operating cost, the ratio between the annual operating costs and the total plant costs is taken as a reference.

Figure 8. Net removal cost of the 2 SMR-DAC designs compared to the 3 reference systems described at the beginning of section 3. The non-energy OPEX includes the fixed *O&M* costs and the cost of replacing and disposing of the sorbent. Powering the DAC with a small modular reactor is considerably cheaper than using a heat pump or enhanced geothermal as heat sources and the grid for electricity. It is, however, slightly more expensive than using the waste heat and electricity from a geothermal power plant.

and maximise the use of nuclear energy. For simplicity, in the rest of the paper, we consider the SMR-DAC-HEI design.
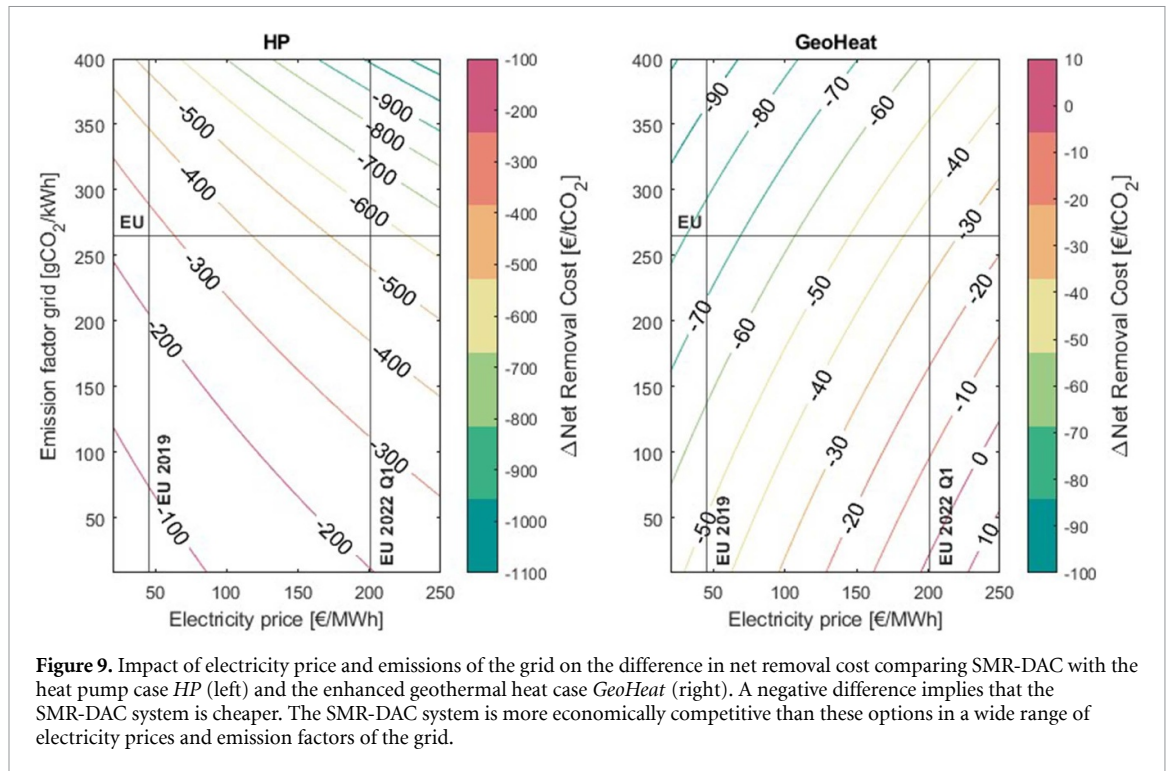
Comparing SMR-DAC-HEI to the other types of plants (figure 8), the SMR-DAC system shows an NRC which is less than half of the NRC when the DAC is powered with an HP. In this case, with the EU average emission factor of 265 gCO_2/kWh [23] the emissions due to the power import from the grid to produce heat and electricity are responsible for an additional cost of 205 €/tCO_2 compared to a fully decarbonized grid. However, even in a zero-carbon grid, removing CO_2 with SMR-DAC would still be 20% cheaper.

Similarly, the SMR-DAC is 14-24% cheaper depending on the emissions from the grid also compared to the *GeoHeat* case, thanks to much lower energy costs. Conversely, when DAC is powered entirely with waste heat and electricity from a flash geothermal power plant (*GeoWaste_el*), the system benefits from the free use of waste heat and the absence of direct CO_2 for the electricity production and shows an NRC of 226 €/tCO_2, 9% lower compared to the HEI system. However, it should be noted that a system of the type *GeoWaste_el* is strongly limited in the scale-up potential by the availability of suitable geothermal power plants. Moreover, such plants can also be characterized by non-negligible CO_2 emissions from the wells, which are not considered here.

The costs obtained in this work are in line with the recent DAC cost estimates [8, 24], and fall in the cost range of 85–510 €/tCO_2 that Young *et al* [25] find for DAC at the giga-tonne scale. For example, McQueen *et al* [8] find a removal cost of 202 €/tCO_2 for DAC coupled with a traditional nuclear reactor, and 193 €/tCO_2 for DAC powered by the waste heat of a geothermal power plant (the equivalent of the case *GeoWaste_el* of this work). However, given the early stage of deployment of DAC, its cost is still highly uncertain and cost estimates differ considerably [25, 26]. Therefore, the significance of the costs obtained in this work should be found more in the consistent comparison of SMR-DAC with other energy supply options, rather than the point values per se.

In this work, we did not include the lifecycle emissions (LCE) of the systems, as they were outside of the boundaries of this research. However, we can derive a first estimation of their impact on the economic performance by looking at large-scale nuclear power plants. The LCE of a pressurized-water reactor (EPR) is in the range of 5–22 gCO_2e/kWh [27]. For the SMR-DAC system, it can be calculated that 1 kWh of electricity from the SMR[10] allows capturing 1.5 $kgCO_2$ and 1.1 $kgCO_2$ in the HEI and LEI design respectively. As such, the LCE of the SMR is expected to be in the order of 1% of the CO_2 that can be removed for a given energy input. This suggests that the impact of the LCE on the NRC is not significant.

---

[10] Including here the direct use of electricity for the DAC and the potential power output lost to supply the required thermal energy to the DAC.

Figure 9. Impact of electricity price and emissions of the grid on the difference in net removal cost comparing SMR-DAC with the heat pump case *HP* (left) and the enhanced geothermal heat case *GeoHeat* (right). A negative difference implies that the SMR-DAC system is cheaper. The SMR-DAC system is more economically competitive than these options in a wide range of electricity prices and emission factors of the grid.

In order to further compare the economic performance of the SMR-DAC system with other options, we analyzed how the difference in NRC varies depending on the electricity price and the emission factor of the grid (see figure 9). For this analysis, we focused only on the system with a relevant scale-up potential. Therefore, we excluded the *GeoWaste_el* option.

An HP-powered DAC is affected more significantly by the electricity price compared to the SMR-DAC system (figure 9) due to the higher use of electricity. In addition to that, the cost difference magnifies as the emission factor of the grid increases as the SMR-DAC has no associated CO_2 emissions. Results show that even in a fully decarbonized grid with very low electricity prices the *HP* case would be still more expensive than SMR-DAC.

As for the *GeoHeat* case, the trend linked to the electricity price is the opposite: higher power costs affect the SMR-DAC system more than *GeoHeat*. This is because, in the SMR-DAC system, the supply of heat comes with a loss in electricity that can be sold to the grid by the SMR, therefore the heat cost is also affected by the electricity prices. As such, it is found that with the (very high) average electricity price of the EU in the first quarter of 2022[11] it would be more cost competitive to remove CO_2 with *GeoHeat* if the electricity grid has an emission factor smaller than around 20 gCO_2/kWh.

3.3. Sensitivity analysis

To understand the possible performance envelop of SMR-DAC, we carried out several sensitivity analyses including: the thermal and energy demand, DAC CAPEX, electricity price, discount rate, and integration cost (i.e. connecting the two plants). Results are shown in figure 10(a).

Looking at the energy-related parameters that can influence the NRC, we find that DAC's energy demand (thermal and electrical) barely influences the NRC. This is possible thanks to the efficient energy use in the SMR-DAC. It also suggests that the results obtained are likely to remain valid for various sorbents and DAC configurations. For the same reason, the electricity price is also found to have a minor effect on the NRC. The interpretation of the consequences of this finding can be twofold. Firstly, the removal cost is stable relative to the market price dynamics. Secondly, the levelized cost of electricity (LCOE) of the SMR does not play a major role in the cost of CO_2 removal. In fact, if we consider the electricity price to correspond to the SMR LCOE (instead of the electricity market price), we see that a 50% increase in the LCOE of the SMR would lead to a 6% increase in the NRC of SMR-DAC. This is particularly relevant given the track record of the nuclear industry in the last 20 years, which has delivered several over-budget projects (specifically, in Europe and the USA) [29].

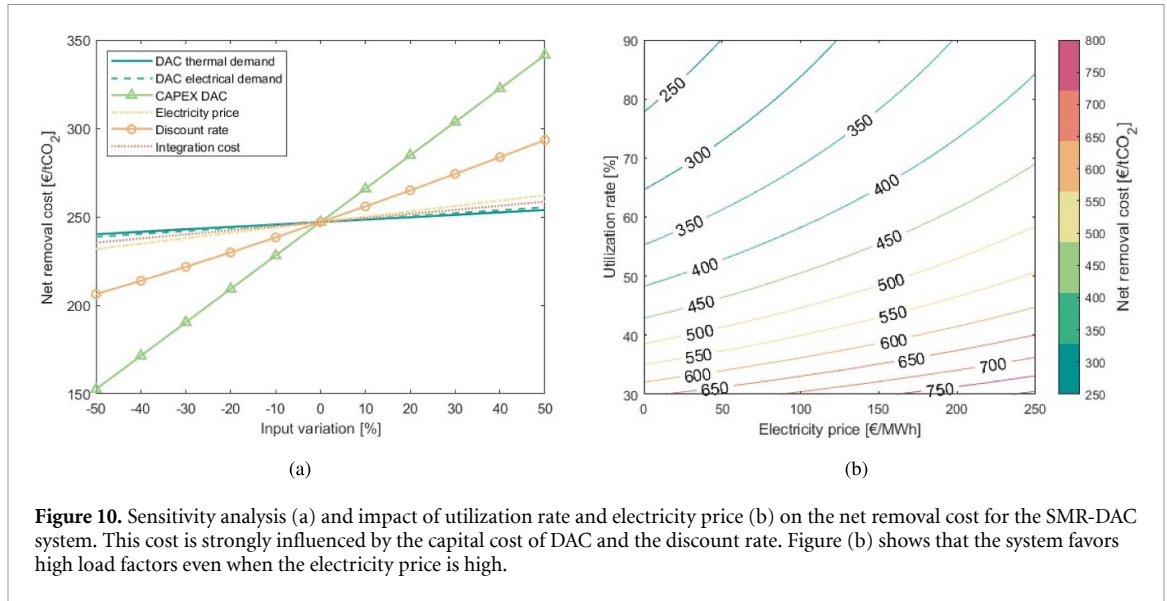---

[11] Standing at 201 €/MWh [28].

Figure 10. Sensitivity analysis (a) and impact of utilization rate and electricity price (b) on the net removal cost for the SMR-DAC system. This cost is strongly influenced by the capital cost of DAC and the discount rate. Figure (b) shows that the system favors high load factors even when the electricity price is high.

On the other hand, while the cost of integration does not play a relevant role in the economics of the system, the CAPEX of DAC has a major impact on the NRC. Given that solid-sorbent DAC is not a mature technology yet, its cost estimations present significant uncertainties ($\pm 50\%$ for the data used in this work [22]) and the NRC values obtained in this work should be interpreted accordingly. For example, a reduction in the CAPEX of 50% brings the NRC from 247 €/tCO$_2$ to 153 €/tCO$_2$; a similar sharp increase in the NRC is observed for a CAPEX increase of 50%. Moreover, as the SMR-DAC system is CAPEX-dominated, the discount rate also plays an important role in the final economics of the system.

Finally, we analyzed the potential trade-off between electricity price and utilization rate of the DAC (percentage of operating hours at full capacity over one year). In figure 10(b) we report a color map of how the NRC changes depending on the utilization rate and electricity price. The figure shows, that the higher the utilization rate, the lower the NRC. Even with extremely high electricity prices, the system should be run at the highest capacity factor possible. At a 90% utilization rate, the NRC remains below 350 €/tCO$_2$ even for electricity prices near 200 €/MWh. On the other hand, if the utilization rate is below 55%, removal costs below 350 €/tCO$_2$ will not be achieved even in the case of free electricity.

4. Scale-up potential and impact of the location

Following the thermodynamic and economic analyses, we wanted to understand the potential role of SMR-DAC in the transition to net zero, both globally and in a few key areas.

4.1. Scale-up potential
First, we estimated the removal potential of the SMR-DAC system in 5 macro-regions: China, India, Europe, South Africa and the United States of America. To do so, we use forecasted SMR installed capacity for each of these regions as developed by the Nuclear Energy Agency (NEA) in [30]. They provide the foreseen SMR capacity installed in these regions in 2035 in low- and high-case scenarios, where the first reflects the possibility that SMRs will show limited levels of cost competitiveness, while the second assumes that SMRs will perform well economically. Considering the optimistic scenario as a reference, the potential for negative emissions Π_j per location j is calculated as

$$\Pi_j = \frac{P_{\text{SMR},j}}{P^{\text{SMR}}_{\text{el,rated}}} \Lambda \tag{3}$$

where $P_{\text{SMR},j}$ is the SMR capacity installed in the location j, $P^{\text{SMR}}_{\text{el, rated}}$ is the rated power output of one SMR module and Λ is the annual carbon removal capacity of the SMR-DAC system per SMR module assuming that the HEI design is implemented. It should be noted that this potential represents an upper bound of the scale-up capacity of the system, and it does not represent a detailed estimation of its future deployments, which depends on multiple factors outside the scope of this work.

Overall, the five locations analyzed have together the potential to remove up to 96 MtCO$_2$/year by 2035. This number is in line with the DAC scale-up required in 2030 according to the Net-Zero by 2050 roadmap
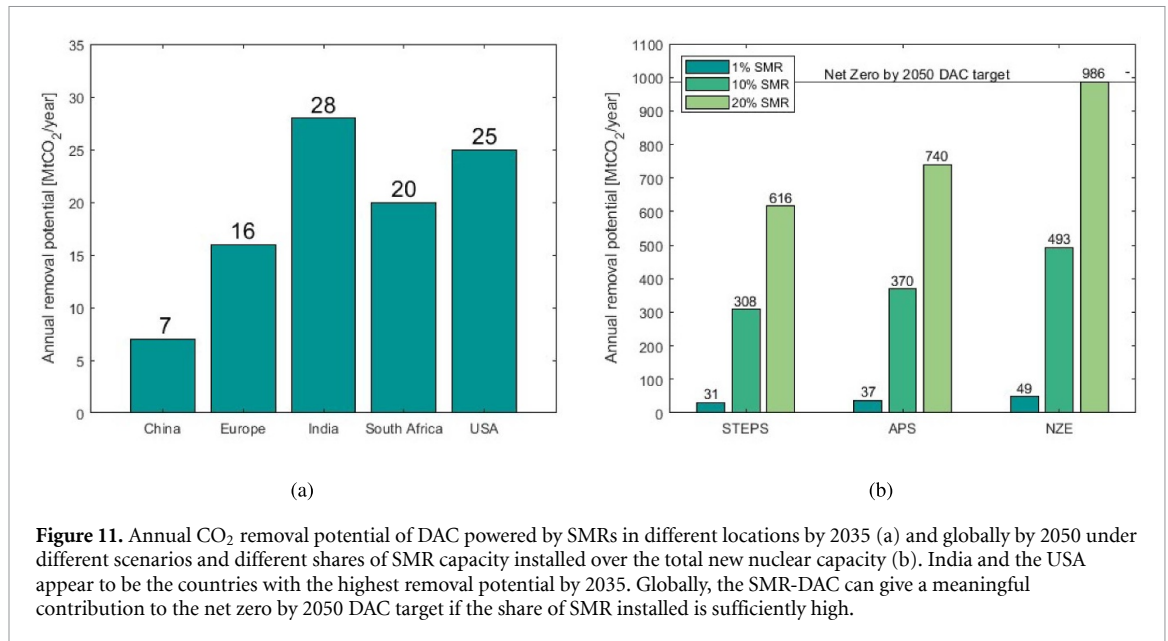
Figure 11. Annual CO_2 removal potential of DAC powered by SMRs in different locations by 2035 (a) and globally by 2050 under different scenarios and different shares of SMR capacity installed over the total new nuclear capacity (b). India and the USA appear to be the countries with the highest removal potential by 2035. Globally, the SMR-DAC can give a meaningful contribution to the net zero by 2050 DAC target if the share of SMR installed is sufficiently high.

Table 4. Power lost if each location would reach its full SMR-DAC (with HEI design) carbon removal potential in 2035.

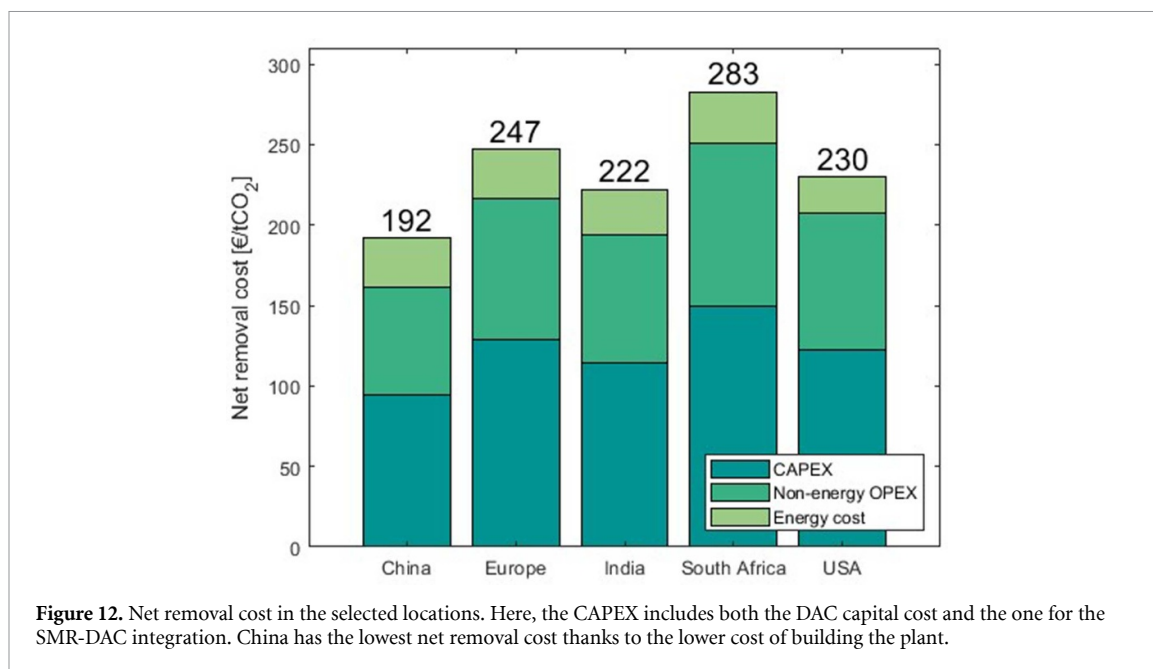|	Power lost (GW)
China	0.6
Europe	1.4
India	2.4
South Africa	1.7
USA	2.1

developed by the IEA [5] (which estimates that a removal capacity of 90 $MtCO_2$/year should be installed globally by 2030). Looking at the different regions, figure 11(a) shows that India and the USA have the highest removal potential, with 28 and 25 $MtCO_2$/year respectively, followed by South Africa and Europe.

Worth noting is that if the future trends for the SMR deployment prove to follow the NEA low-case scenario instead of the high-case, the annual removal potential of the SMR-DAC system would fall to 4 $MtCO_2$/year (96% lower). However, considering the results of this study, DAC could significantly contribute to the deployment of SMR, as it allows to decouple the SMR performance from the characteristics of the electricity market. In other words, beyond a certain negative emission price, the SMR-DAC would make more profit from providing negative emissions credits than from selling electricity (a similar case exists for bioenergy, and is known as the Aines principle [31]). At the same time, it is worth mentioning that the negative emission credits are highly policy-dependent, which could put constraints on the development of SMR-DAC systems in certain locations.

Furthermore, considering the potential, it is assumed that all the SMRs available are equipped with DAC. As such, a significant portion (59% for the HEI design, 76% for the LEI) of the power from the SMR would be unavailable for electricity use. Specifically, the loss ranges from 0.6 GW of capacity in China to 2.4 GW in India (see table 4). The impact of this loss might be negligible for countries like China, the USA and Europe, where the installed power capacity is in the order of thousands on GW [32]. However, it may be problematic for countries like South Africa, where a loss of 1.7 GW represents 3% of the power installed in 2020 [32]. In any case, it is important to point out that the power that is dedicated to the DAC should be replaced with other energy sources or further deployment of SMRs.

The estimation for the SMR-DAC potential can be projected to 2050 if we broaden the potential at a global scale, where scenarios were recently presented in the World Energy Outlook 2022 developed by the IEA [33]:

- Stated policies scenario (STEPS), which looks at what governments 'are actually doing to reach the targets and objectives that they have set out'
- Announced pledges scenario, which 'assumes that governments will meet, in full and on time, all of the climate related commitments that they have announced'
- Net zero emissions by 2050 (NZE) Scenario, which 'sets out a pathway to the stabilization of global average temperatures at 1.5 °C above pre industrial levels'

Figure 12. Net removal cost in the selected locations. Here, the CAPEX includes both the DAC capital cost and the one for the SMR-DAC integration. China has the lowest net removal cost thanks to the lower cost of building the plant.

From these scenarios, we retrieved the projections of the new nuclear capacity installed by 2050. We assumed different shares of SMRs to obtain the potential installed capacity of SMR, and thus the removal potential of SMR-DAC (again, interpreting this as an upper bound of the scale-up potential).

Assuming different shares of SMR in the future installed nuclear capacity, it can be noticed that a global removal capacity of hundreds $MtCO_2$/year could be achieved in all the three scenarios (figure 11(b)) even with a relatively low share of SMR (10%). When the share is 20%, 616 $MtCO_2$/year could be removed in the STEPS scenario, and almost to 1 $GtCO_2$/year in the NZE scenario. If SMR do not prove to be an attractive solution reaching only 1% of the installed nuclear capacity, the removal capacity of SMR-DAC drops to a few tens $MtCO_2$/year, which might however worth pursuing given the challenges of integrating DAC in the energy system.

To scale up the carbon removal via DAC, a necessary condition is the presence of geologic CO_2 storage sites. While this is a factor that should be carefully considered when developing specific projects, on a regional level this is unlikely to be a limiting factor for the deployment of carbon removal via DAC. In fact, in the considered regions the storage capacity ranges from hundreds to several thousand $GtCO_2$ [34].

4.2. Impact of the location on the NRC

To estimate the impact of the location on the NRC, for each of the five regions mentioned above, we recalculate the NRC according to the local electricity price and the location factor (which reflects the impact of the location on the capital cost of the system). More details are in the supplementary information.

Analyzing the NRC in each location (figure 12), China appears to be the most economically competitive, with an NRC of 192 €/tCO_2. This is mainly driven by a very low location factor, which reduces the capital and the O&M cost by 30%. On the other hand, a high location factor makes South Africa the most expensive region among the ones analyzed. The price of electricity does not play a big role in the cost differences for two main reasons: (1) DAC is a capital-intensive technology, (2) the energy demand for DAC is mostly thermal, and heat is supplied efficiently from the SMR, thus reducing the electrical power loss.

Overall, looking at the potential and the NRC together, India and the USA appear to be the most attractive locations for high removal capacities with SMR-DAC at a competitive cost. However, it should be noted that these two factors alone are not sufficient to determine the attractiveness of a region. Multiple other factors, such as the cost of capital, local policies and the environmental conditions [35, 36] can have a significant impact on the removal cost of DAC.

5. Discussion

While the coupling of DAC and SMR appears attractive from a techno-economic perspective, it will present additional challenges—not necessarily technical—which are common to any technology linked to nuclear energy. First, the implementation of such integration will require the identification of any specific regulatory requirements that might be requested by national nuclear agencies. In this regard, SMR-DAC plants could

build upon the knowledge of coupling nuclear plants with district heating [37]. Second, societal acceptance might become a barrier to large-scale deployment, especially in Europe. Third, long-term plant decommissioning and ownership would have to be tackled (but this would apply equally to SMR and SMR-DAC plants).

From a methodological perspective, the analysis presented in this work, which aims at providing a first estimate of the SMR-DAC system, could be extended and further improved by tackling a few factors. First, it should be noted that the analysis in this work is static, meaning that we exclude the time variable, for example in the electricity prices. While a static techno-economic analysis allows for a clear comparison between different DAC energy supplies, it does not capture the complexity and the trade-offs that a real-world plant would face. Specifically, there are two major points where the static analysis performed falls short.

The first one is the assumption that the ambient conditions remain constant, which implies fixed energy demand and removal capacity of the DAC. However, the energy requirements and the productivity of solid sorbent DAC modules are strongly affected by the ambient temperature and humidity, with the energy demand increasing with higher temperature and the productivity increasing with higher humidity [35]. In addition, the electric power output of the SMR is also influenced by the ambient temperature, typically showing a 0.5% decrease per 1 °C increase [38]. These variations can affect the design of the system by e.g. (i) reducing the maximum number of DAC modules that can be powered by the SMR system and (ii) changing the mass flows required per stream in the HEI design.

The second consequence is that the analysis does not consider the electricity price over time. While this factor will not influence the design of the system, the dynamic nature of electricity prices may play a role in how the SMR-DAC system is operated. In particular, depending on the electricity price and the negative emission price, the SMR-DAC system could decide if it is more profitable to deliver additional electricity or enable negative emissions.

Overall, a dynamic analysis of the system that includes the variation of ambient conditions and the electricity prices over time is necessary to understand how the SMR-DAC could be operated in a realistic environment and to improve the accuracy of the economic assessment of the system.

6. Conclusion

In conclusion, this study presents a comprehensive analysis of the integration of SMRs with solid sorbent DAC. The findings highlight the significant potential of coupling SMRs with DAC, resulting in a substantial increase in the utilization of thermal energy from the nuclear reactor (from 32% to 76%–85%). The proposed integration designs showed that a 50-MW SMR equipped with DAC could remove approximately 0.3 $MtCO_2$ annually, while still maintaining a net electrical power output of 12–21 MW.

From a techno-economic standpoint, the SMR-DAC system offers a cost-effective, competitive solution compared to other alternatives such as DAC powered by a high-temperature HP or a dedicated geothermal heating system. Although the integration of DAC with waste heat from a geothermal power plant would be slightly cheaper than the SMR-DAC system, the SMR-DAC allows for overcoming the limitations associated with the regional or national availability of geothermal waste heat at a sufficiently high temperature.

Moreover, the study assesses the potential for future deployment of SMR-DAC systems in various regions, including China, Europe, India, South Africa, and the USA. The analysis indicates that the scale-up potential of SMR-DAC could be up to around 96 $MtCO_2$/year by 2035, aligning with the required negative emissions from DAC outlined in the Net Zero by 2050 roadmap proposed by the IEA. Additionally, the impact of regional differences on the removal cost is evaluated, finding that China has the lowest removal cost thanks to the lower cost of building the plant.

Overall, the findings of this study highlight the promising potential role of SMR-DAC systems in advancing the transition towards a net-zero world. The integration of scalable, low-carbon energy sources such as SMRs with DAC holds significant potential for contributing to global climate objectives and achieving substantial CO_2 removal at a reasonable cost.

Data availability statement

All data that support the findings of this study are included within the article (and any supplementary files).

Acknowledgments

Conflicts of interest

The authors declare that they have no known competing financial interests or personal relationships that could have appeared to influence the work reported in this paper.

Contributions

Luca Bertoni: Conceptualization, Methodology, Software, Formal analysis, Data curation, Visualization, Writing—Original Draft

Simon Roussanaly: Methodology, Supervision, Funding acquisition, Writing—Review & Editing

Luca Riboldi: Supervision, Validation, Writing—Review & Editing

Rahul Anantharaman: Writing—Review & Editing

Matteo Gazzani: Conceptualization, Methodology, Visualization, Supervision, Writing—Review & Editing

ORCID iD

Matteo Gazzani https://orcid.org/0000-0002-1352-4562

References

[1] Marcucci A, Kypreos S and Panos E 2017 The road to achieving the long-term Paris targets: energy transition and the role of direct air capture *Clim. Change* **144** 181–93

[2] Rogelj J *et al* 2018 Scenarios towards limiting global mean temperature increase below 1.5 °C *Nat. Clim. Change* **8** 325–32

[3] National Academies of Sciences, Engineering, Medicine 2019 *Negative Emissions Technologies and Reliable Sequestration: A Research Agenda* (The National Academies Press) (https://doi.org/10.17226/25259)

[4] Fuss S *et al* 2018 Negative emissions-part 2: costs, potentials and side effects *Environ. Res. Lett.* **13** 063002

[5] IEA 2021 Net zero by 2050 a roadmap for the global energy sector *Technical Report*

[6] Carbon Engineering 2021 Direct air capture technology (available at: https://carbonengineering.com/our-technology/)

[7] Climeworks 2021 The next step towards a climate-positive world: Orca! (available at: https://climeworks.com/roadmap/orca)

[8] McQueen N *et al* 2020 Cost analysis of direct air capture and sequestration coupled to low-carbon thermal energy in the United States *Environ. Sci. Technol.* **54** 7542–51

[9] IEA 2022 Nuclear power and secure energy transitions. From today's challenges to tomorrow's clean energy systems *Technical Report* (available at: www.iea.org/t&c/)

[10] D. o. N. P. IAEA 2020 Advances in small modular reactor technology developments, A Supplement to: IAEA Advanced Reactors Information System (ARIS) 2020 edn 354

[11] I. E. Agency 2019 The future of hydrogen

[12] Lechtenböhmer S, Nilsson L J, Åhman M and Schneider C 2016 Decarbonising the energy intensive basic materials industry through electrification - implications for future eu electricity demand *Energy* **115** 1623–31

[13] Pilorgé H, Psarras P, He J and Wilcox J 2019 Combining geothermal potential and direct air capture for negative emission power generation in California *Geothermal, Trans. - Geothermal Resources Council, Geothermal Resources Council* pp 462–8

[14] Adams B, Sutter D, Mazzotti M and Saar M O 2020 *Combining Direct air Capture and Geothermal Heat and Electricity Generation for net-Negative Carbon Dioxide Emissions* (ETH Zurich) p 38018

[15] Slesinski D and Litzelman S 2021 How low-carbon heat requirements for direct air capture of CO_2 can enable the expansion of firm low-carbon electricity generation resources *Front. Clim.* **3** 728719

[16] Stauff N E, Mann W N, Moisseytsev A, Durvasulu V, Mantripragada H and Fout T 2023 Assessment of nuclear energy to support negative emission technologies

[17] Energy.gov. 2023 NRC certifies first U.S. small modular reactor design

[18] USNRC 2020 Application documents for the nuscale design (available at: www.nrc.gov/reactors/new-reactors/smr/nuscale/documents.html)

[19] NuScale LCC 2018 Chapter ten, steam and power conversion system, *Technical Report*

[20] NuScale LCC 2022 Technology overview (available at: www.nuscalepower.com/technology/technology-overview)

[21] Sabatino F, Grimm A, Gallucci F, van Sint Annaland M, Kramer G J and Gazzani M 2021 A comparative energy and costs assessment and optimization for direct air capture technologies *Joule* **5** 2047–76

[22] Valentine J and Zoelle A 2022 Direct air capture case studies: sorbent system

[23] European Environment Agency 2022 Greenhouse gas emission intensity of electricity generation in Europe (available at: www.eea.europa.eu/ims/greenhouse-gas-emission-intensity-of-1)

[24] Wijesiri R P, Knowles G P, Yeasmin H, Hoadley A F A and Chaffee A L 2019 Technoeconomic evaluation of a process capturing CO_2 directly from air *Processes* **7** 503

[25] Young J, McQueen N, Charalambous C, Foteinis S, Hawrot O, Ojeda M, Pilorgé H, Andresen J, Psarras P, Renforth P and van der Spek M 2022 The cost of direct air capture and storage: the impact of technological learning, regional 2 diversity, and policy

[26] Chauvy R and Dubois L 2022 Life cycle and techno-economic assessments of direct air capture processes: an integrated review

[27] Hill N 2013 Current and future lifecycle emissions of key 'low carbon' technologies and alternatives final report

[28] European Commission 2022 Quarterly report on European Electricity Market *Technical Report*

[29] Stewart W R and Shirvan K 2022 Capital cost estimation for advanced nuclear power plants *Renew. Sust. Energy Rev.* **155** 111880

[30] Lokhov A, Sozoniuk V and Rothwell G 2016 Small modular reactors: nuclear energy market potential for near-term deployment *Nucl. Dev.* **143** 75

[31] Sandalow D, Aines R, Friedmann J, Mccormick C and Sanchez D L 2021 Biomass carbon removal and storage (BICRS) roadmap

[32] Country Economy, Electricity Generation 2021 (available at: https://countryeconomy.com/energy-and-environment/electricity-generation)

[33] IEA 2022 World energy outlook 2022 *Technical Report*

[34] Kearns J, Teletzke G, Palmer J, Thomann H, Kheshgi H, Chen Y H H, Paltsev S and Herzog H 2017 Developing a consistent database for regional geologic CO_2 storage capacity worldwide *Energy Proc.* **114** 4697–709

[35] Wiegner J F, Grimm A, Weimann L and Gazzani M 2022 Optimal design and operation of solid sorbent direct air capture processes at varying ambient conditions *Ind. Eng. Chem. Res.* **61** 12649–67

[36] Sendi M, Bui M, Dowell N M and Fennell P 2022 Geospatial analysis of regional climate impacts to accelerate cost-efficient direct air capture deployment *One Earth* **5** 1153–64

[37] Oliker I 2022 District heating supply from nuclear power plants

[38] Linnerud K, Mideksa T K and Eskeland G S 2011 The impact of climate change on nuclear power supply *Energy J.* **32** 149–68